# Nonlinear Spectroscopy of Alkali Atoms in Cold Medium of Astrophysical Relevance

**Dmitry K. Efimov [1,2], Martins Bruvelis [3], Nikolai N. Bezuglov [1], Milan S. Dimitrijević [4,5,6], Andrey N. Klyucharev [1], Vladimir A. Srećković [7,*], Yurij N. Gnedin [8] and Francesco Fuso [9]**

[1] Saint Petersburg State University, St. Petersburg State University, 7/9 Universitetskaya nab., St. Petersburg 199034, Russia; dmitry.efimov@uj.edu.pl (D.K.E.); bezuglov50@mail.ru (N.N.B.); anklyuch@gmail.com (A.N.K.)

[2] Instytut Fizyki im. Mariana Smoluchowskiego, Uniwersytet Jagielloński, 30-348 Kraków, Poland

[3] Laser Centre, University of Latvia, LV-1002 Riga, Latvia; martins.bruvelis@gmail.com

[4] Astronomical Observatory, Volgina 7, 11060 Belgrad, Serbia; mdimitrijevic@aob.rs

[5] IHIS-Technoexperts, Bezanijska 23, 11080 Zemun, Serbia

[6] Observatoire de Paris, 92195 Meudon CEDEX, France

[7] Institute of Physics, University of Belgrad, P.O. Box 57, 11001 Belgrad, Serbia

[8] Pulkovo Observatory, Russian Academy of Sciences, St. Petersburg 196140, Russia; gnedin@gao.spb.ru

[9] Dipartimento di Fisica Enrico Fermi and CNISM, Università di Pisa, I-56127 Pisa, Italy; francesco.fuso@unipi.it

*** Correspondence: vlada@ipb.ac.rs; Tel.: +381-(0)11-37-13-000**

**Abstract:** The time-dependent population dynamics of hyperfine (HF) sublevels of $n^2p_{3/2}$ atomic states upon laser excitation in a cold medium of alkali atoms is examined. We demonstrate some peculiarities of the absorption HF multiplet formation in $D$2-line resulting from a long interaction time ($\sim$200 μs) interaction between light and Na ($n = 3$) and Cs ($n = 6$) atoms in a cold and slow sub-thermal ($T \sim$ 1K) beam. We analytically describe a number of $D$2-line-shape effects that are of interest in spectroscopic studies of cold dusty white dwarfs: broadening by optical pumping, intensity redistribution within components of $D$2-line HF multiplet for partially closed transitions and asymmetry of absorption lines induced by AC Stark shifts for cyclic transitions.

**Keywords:** spectroscopy; alkali atoms; astrophysics

---

## 1. Introduction

Investigation of the fluorescence spectrum of sodium atoms is an important data source for astrophysics and, especially, for understanding the physical processes in cool stars, namely, for brown and white dwarfs. For example, the measured precise atmospheric parameters for shortest period binary white dwarfs confirm the existence of metal-rich envelopes around extremely low-mass white dwarfs and allow us to examine the distribution of the abundance of non-hydrogen elements, including Na, as a function of effective temperature and mass [1]. It is worth emphasizing that we can expect the gravitational wave strain for such systems.

Other interesting astrophysical objects are metal polluted white dwarfs and dusty white dwarfs. It has long been suspected that metal polluted white dwarfs (types DAZ, DBZ and DZ) and white dwarfs with dusty disks can possess planetary systems [2]. Therefore, the spectroscopic observations of sodium atoms in these objects can confirm the validity of this hypothesis. It is in fact known that all dusty white dwarfs show evidence for alkali atoms accretion onto their dusty disk.

In reference [3], the observational constraints on the origin of metals and alkali atoms in cool white dwarfs are discussed. The presence of absorption lines of Na, Mg, Fe etc in the photospheres of

cool hydrogen atmosphere DA-type white dwarfs has been an unexplained problem for a long time. However, in [4], it was shown that the metal abundances in the atmospheres of white dwarfs can be explained by episodic accretion events whenever the white dwarf travels through relatively overdense clouds.

Furthermore, Na 8183.27, 8192.81 Å absorption doublet was discovered in astrophysical systems of white dwarf–main sequence binaries. It allows us to investigate in detail the process of mass transfer interaction in these complex astrophysical systems.

In astrophysics, there is a wide interest in the search for dusty white dwarfs with powerful infrared excess. This excess is produced by orbiting dust disk that contains planetary systems and planetesimals. All these materials get accreted onto the white dwarf and enrich its pure hydrogen or/and helium atmosphere. Studying these heavy elements enriched white dwarfs becomes an effective way to measure directly the bulk compositions of extrasolar planetesimals [5]. Na atoms can be the essential part of these heavy-element clouds; therefore, detailed knowledge of Na emission features can be extremely relevant for investigating such astrophysical problems.

Recently, combined Spitzer and ground-based Korea Microlensing Telescope Network observations identified and precisely measured an Earth-mass planet orbiting ultra cool dwarf [6]. Observations of Na atoms in ultra cool dwarfs can become the effective method for determining planetesimals and Earth-mass planets in dusty disks surrounding the central ultra cool dwarf.

We note as well that, already in 1974, Brown [7] detected the first neutral sodium cloud near Jovian satellite Io (see also [8]). The investigation of these sodium clouds is needed for better understanding of the interaction between Io's atmosphere and Jovian magnetosphere [9] and of processes in the Jovian environment [10].

We are concerned here with important particularities of cold alkali atoms absorption spectra in D2-lines (see Figure 1) that result from a long interaction time of light and matter and, as a consequence, from a strong involvement of optical pumping phenomena within hyperfine (HF) components of the ground and excited states. The described novel theoretical predictions are compared with experimental data obtained in sub-thermal (cold) atomic beams [11,12] operated with two different alkali species, namely Na and Cs. Atomic units are used unless stated otherwise.
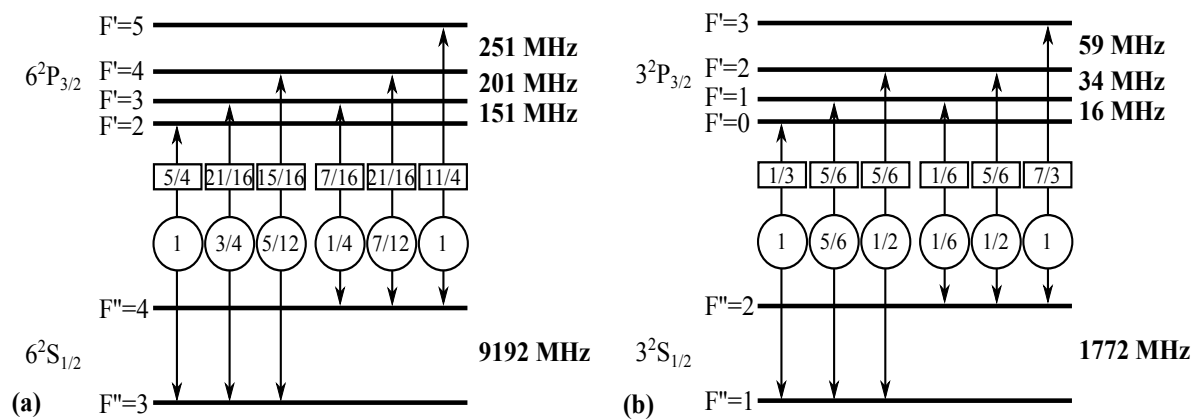


**Figure 1.** Transition strength $\tilde{S}_{F''F'}$ (boxed) and branching $\Pi$ (circled) factors for the hyperfine components of $D$2-lines for (**a**) cesium (transition $6^2s_{1/2} \to 6^2p_{3/2}$) and (**b**) sodium (transition $3^2s_{1/2} \to 3^2p_{3/2}$) atoms. For cyclic (closed) transitions, the factor $\Pi = 1$. The natural lifetime $\tau$ and saturation threshold $\Omega_{st} = 1/(\tau\sqrt{2})$ of the resonance states are $\tau = 30.5$ ns and $\Omega_{st} = 3.7$ MHz for Cs while $\tau = 16.4$ ns and $\Omega_{st} = 6.9$ MHz for Na, respectively.

## 2. Formation of HF Absorption Multiplet for Partially Open Transitions

Absorption spectra of alkali atoms have a multiplet form due to HF structure of atomic states (see Figure 1). There are two different classes of multiplet components corresponding to cyclic

(or closed) and partially open (or non-cyclic) transitions between HF sublevels $F'$ and $F''$ of the resonant excited (e) and the ground (g) states, respectively. In the partially open case, each spontaneously emitted photon induces two transitions $F' \rightarrow F'' = 2,1$ in Na and $F' \rightarrow F'' = 4,3$ in Cs with probabilities $\Pi$ (see Figure 1). The dimensionless parameter $\Pi$ is called the branching ratio. The cyclic transitions correspond to $\Pi = 1$ and they are particularly important in cooling and trapping techniques of neutral atoms, for example, in magneto-optical traps (MOTs) [13].

Excitation of the partially open individual transition $F'' \rightarrow F'$ is accompanied by optical pumping phenomenon that is usually associated with redistribution of population within HF sublevels of the ground state because of interaction with resonant light fields [14]. Line-shape effects due to optical pumping (the so-called depletion broadening) in the weak excitation limit and long interaction time $\tau_{tr}$ were examined in detail in [15]. A convenient approximation in describing the time-dependent population dynamics of HF sublevels $F'', F'$ is a two-level model. Atoms are excited on the atomic transition by monochromatic laser radiation with frequency $\omega_L$, amplitude $A_0$, and detuning $\delta \equiv \omega_L - \omega_{eg}$. If the laser intensity is insufficient to saturate the transition, which corresponds to Rabi frequency $\Omega$ ($\Omega = \langle e| A_0 \hat{d} |g\rangle$, where $\hat{d}$ is the atomic dipole operator) being below the natural linewidth $\Gamma_e$ of the excited state, then the rate of spontaneous transitions per one atom is equal to [14]:

$$\Gamma_g = \frac{\Omega^2 \Gamma_e}{4\delta^2 + \Gamma_e^2}; \quad \Omega \ll \Gamma_e. \tag{1}$$

In a partially open system, each spontaneously emitted photon returns to g-state the $\Pi$-portion of the population, while the remaining $(1-\Pi)$-portion is transferred to states outside the two-level system. It means the depletion rate $\Gamma_{pum}$ is equal to $\Gamma_{pum} = (1-\Pi)\Gamma_g$ and the lower state population $n_g$ of the atom decays exponentially $n_g(\tau) \approx \exp(-\tau/\tau_{pum})$ at the time $\tau$ upon transit through the laser beam. The corresponding pumping time is $\tau_{pum} = 1/\Gamma_{pum}$, i.e.,

$$\tau_{pum} = \frac{1}{\Gamma_{pum}} = \frac{1}{1-\Pi} \frac{4\delta^2 + \Gamma_e^2}{\Omega^2 \Gamma_e}. \tag{2}$$

In experiments involving atom beams crossed by the laser radiation [11,12], we can identify a transit time $\tau_{tr}$. In such conditions, the total population after the atom beam has crossed the laser radiation, $n_g(\infty)$, becomes $n_g(\infty) \approx \exp(-\tau_{tr}/\tau_{pum})$. Thus, the criterion for the development of optical pumping is $\tau_{tr} > \tau_{pum}$, or in terms of Rabi frequencies

$$\Omega > \Omega_{cr}; \quad \Omega_{cr} = \Gamma_e \sqrt{\frac{1 + 4\delta^2/\Gamma_e^2}{1-\Pi} \cdot \frac{\tau_e}{\tau_{tr}}}, \tag{3}$$

where $\tau_e = 1/\Gamma_e$ is the radiative lifetime of the upper e-state. The ratio $\tau_e/\tau_{tr}$ for cold atomic beams acquires values of $\sim 10^{-4}$ ($\tau_e \approx 20$ ns, $\tau_{tr} \approx 200$ μs) [3]. Therefore, the depletion manifestation can be observed at Rabi frequencies well below (by two orders of magnitude) the saturation frequency $\Omega_{st} \equiv \Gamma_e/\sqrt{2}$; exceeding this value results in the development of nonlinear (power broadening) and quantum optics effects [14].

Important spectroscopic features of optical pumping emerge when the Rabi frequency is set close, or above, the critical value $\Omega_{cr}$ (3) [15]. Conventional experiments would usually register the fluorescence signal $J$ (absorption line) from the entire excitation volume, which is proportional to the total number $\Gamma_e \bar{n}_e$ of photons emitted by a single atom. On the other hand, the number $(1-\Pi)\Gamma_e \bar{n}_e$ of spontaneously emitted photons on transitions outside the g-e system is equal to the total loss $1 - n_g(\infty)$ of the ground state population, so that the signal $J$ can be written as

$$J \equiv \Gamma_e \bar{n}_e = \frac{1}{(1-\Pi)} \left(1 - \exp(-\tau_{tr}/\tau_{pum})\right). \tag{4}$$

Equation (4) yields a dependence of the fluorescence signal on the laser detuning $\delta$ in the following explicit form:

$$J(\delta) = \frac{\Omega^2 \tau_{tr}}{\Gamma_e} \frac{1}{P_{pum}} \left[1 - \exp\left(-\frac{P_{pum}}{1 + 4\delta^2/\Gamma_e^2}\right)\right],\tag{5}$$

$$P_{pum} = \frac{\tau_{tr}}{\tau_{pum}^0}; \quad \tau_{pum}^0 = \frac{1}{1 - \Pi} \frac{\Gamma_e}{\Omega^2}.\tag{6}$$

The above equation and data presented in Figure 2 show that the absorption spectrum strongly depends on the pumping parameter $P_{pum}$ defined as in Equation (6), which is given by the ratio of transit time $\tau_{tr}$ and pumping time $\tau_{pum}^0$. The latter has the meaning of optical pumping time at resonant excitation, when $\delta = 0$. Importantly, the parameter $P_{pum}$ can be large even at laser intensities well below the saturation limit: $P_{pum} >> 1$ when $\tau_{tr} >> \tau_{pum}^0$ and $\Omega << \Omega_{cr}$.
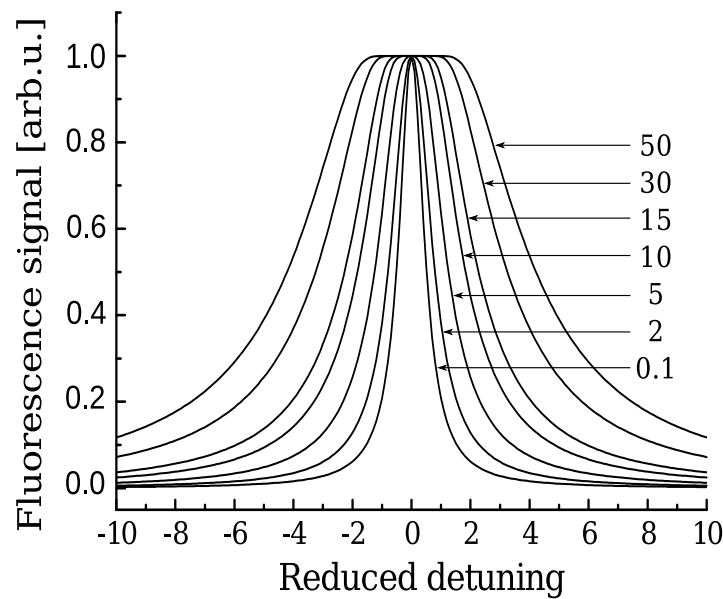


**Figure 2.** Dependence of the absorption signal $J$ Equation (5) on the reduced detuning $\delta/\Gamma_e$ for different values of the pumping parameter $P_{pum}$ Equation (6) (shown as labels of the curves). All curves are unity-normalized at the line center $\delta = 0$.

According to Equation (4), optical pumping leads to saturation of the fluorescence signal at the value of $1/(1 - \Pi)$. This fact along with redistribution of intensities within *D*2-line multiplet have been predicted and experimentally demonstrated in [15]. Another phenomenon described by Equations (4) and (5) is related to depletion broadening of the absorption line. As an estimation of the characteristic full width $\Delta_{pm}$ of the spectral absorption profile induced by optical pumping, one can write

$$\Delta_{pm} = \sqrt{\frac{\tau_{tr}}{\tau_e}(1 - \Pi) \cdot \Omega^2 - \Gamma_e^2}.\tag{7}$$

In the case of cold beams of alkali atoms, with $\tau_{tr}/\tau_e \sim 10^4$ and $\Omega > \Omega_{cr}$ for $\delta = 0$ (see Equation (3)), the width $\Delta_{pm}$ acquires the form $\Delta_{pm} \approx \Omega\sqrt{(1 - \Pi)\tau_{tr}/\tau_e} \sim 100 \cdot \Omega$, which may essentially exceed the power broadening effects ($\Delta_{pw} \sim \Omega$) even in the limit of weak excitation. The corresponding experimental investigation of spectral broadening due to optical pumping (the parameter $\tau_{tr}/\tau_e \sim 100$) in partially open HF level systems in Na has been reported in [15]. We note that, since the experiments were performed at low number densities ($\sim 10^{10}$ cm$^{-3}$) of Na atoms, line-shape modifications by radiation trapping in collimated beams [16] can be disregarded.

### 3. Experimental Setup and Spectroscopic Data

Common experimental practice foresees the use of two types of thermal beams: effusive beam with longitudinal velocity $v_{lg} \approx 400$ m/s [17], and crossed beams with $v_{lg} \approx 600$ m/s [18]. The second type represents a supersonic beam with $v_{lg} \approx 1100$ m/s [15] and a rather specific velocity distribution function [19]. An additional experimental possibility is represented by laser cooled atomic beams [20,21], which are characterized by small $v_{lg}$ around 12 m/s, which corresponds to the sub-thermal temperature interval lying below 1 K and practically negligible transversal velocity.

At the core of the relevant setup is a hollow pyramid with reflective inner surfaces and a hole at its vertex. By shining a single, large diameter (35 mm) laser beam along the pyramid axis, the optical configuration of an MOT is achieved. Imbalance of the radiation pressure along the pyramid axis pushes Cs atoms out of the pyramid hole. Further collimation of the atoms is achieved by a transverse optical molasses right after the pyramid hole (Figure 3). The atom beam is then excited by a diode laser tunable over the hyperfine transitions belonging to the *D*2-line of Cs; blue laser radiation is superposed in order to ionize the excited atoms. The production rate of ions is proportional to the total number of excited atoms in the excitation volume. Ions are effectively collected and detected, providing a sensitive probe of the excited population [12]. Note that line-shape modifications by radiation trapping in a cold medium [22,23] can be disregarded for the above experimental conditions.
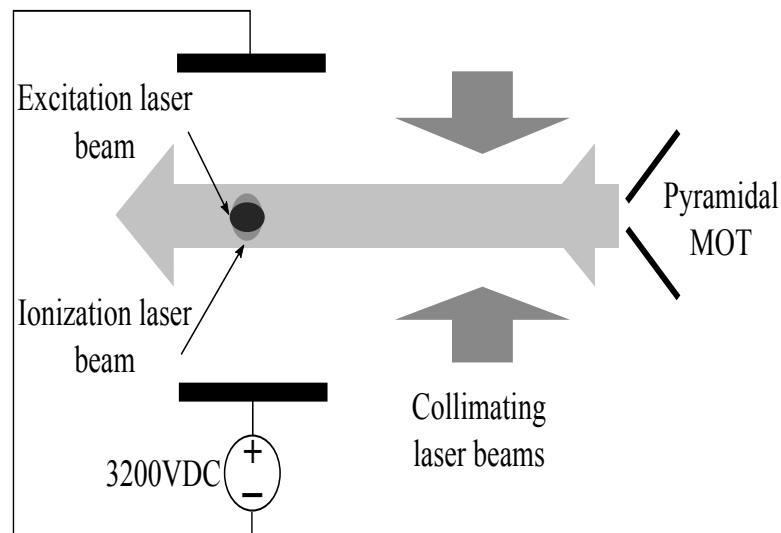


**Figure 3.** Schematic diagram of the experimental setup for the production and excitation of a cold Cs atom beam.

Figure 4 shows an experimentally obtained absorption profile (dots) upon excitation of the cyclic $F'' = 4 \rightarrow F' = 5$ transition for Cs atoms. We underline two main points: (i) although the main line-profile results from symmetric power broadening; (ii) there is a slight asymmetry in the line-shape.

This asymmetry is induced by the other HF components of $n^2 p_{3/2}$ sublevels and, as it will be shown in the next section, is strongly affected by the relationships between laser Rabi frequency and values of HF splitting. For comparison, we show in Figure 5 a situation occurring for Na atoms in similar experimental conditions to demonstrate the occurrence of a quite non-standard line shape, whose explanation is presented in the following.
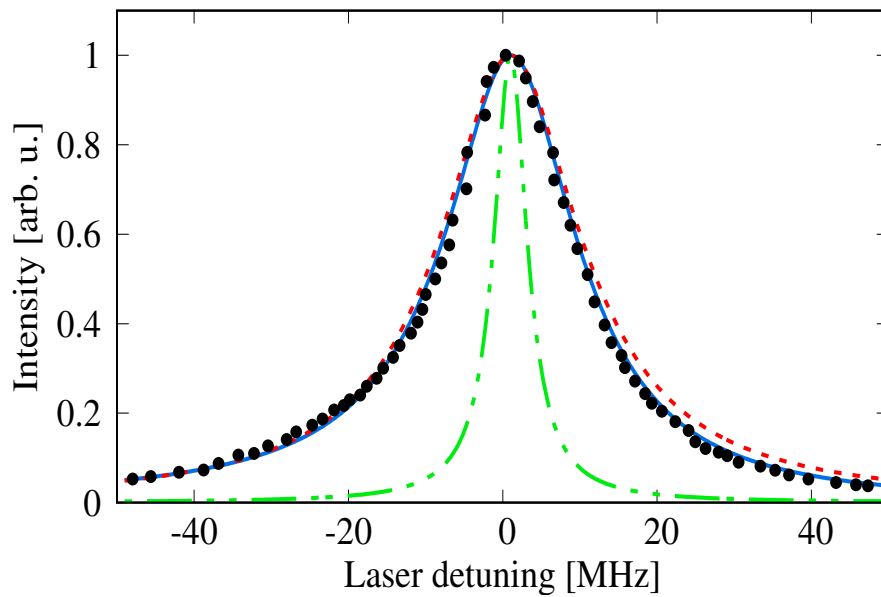
**Figure 4.** Theoretical (solid curve, Equation (19)) and experimental [11] (dots) absorption profile of the $D2$-line of Cs upon an excitation of the closed $F'' = 4 \rightarrow F' = 5$ transition in a cold sub-thermal Cs beam for laser power of 1.0 mW (the corresponding Rabi frequency $\Omega = 21.2$ MHz). The dashed curve corresponds to the power broadening profile. The bar-dashed curve exhibits the natural broadening profile.
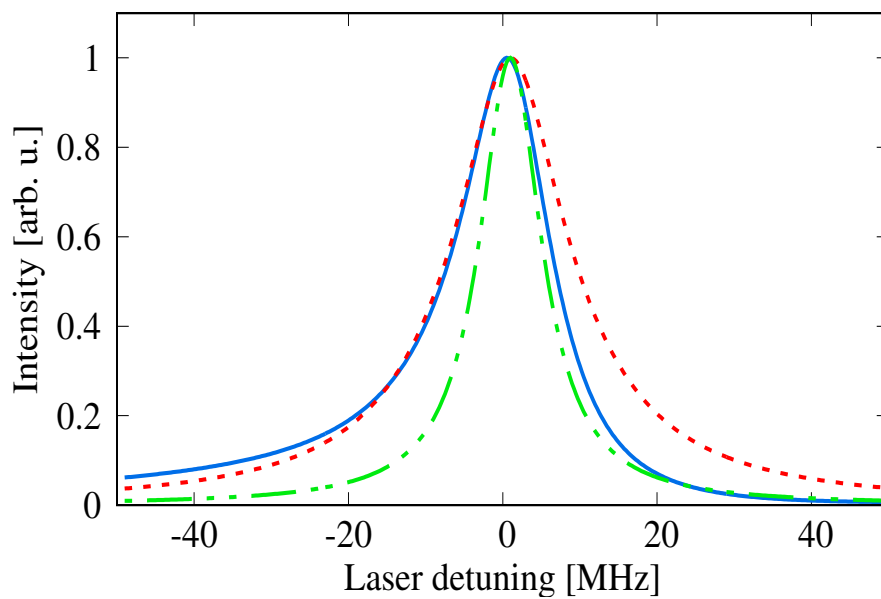


**Figure 5.** The same as in Figure 4 in the case of $D2$-line of sub-thermal Na atoms and the excitation of the closed $F'' = 2 \rightarrow F' = 3$ transition with laser Rabi frequency $\Omega = 21.2$ MHz.

## 4. Cyclic Transitions Treatment: Modeling and Discussion

The description of cyclic transitions can rarely be reduced to the two-level system model: even upon resonant excitation ($\delta = 0$) in a cold beam, the presence of other HF levels may result in the appearance of fundamentally new effects. Let us add the third level $|3\rangle$ to a two-level closed system $|4\rangle$, $|2\rangle$ (see Figure 6a), which can decay to the passive state $|1\rangle$ due to spontaneous emission.

We associate states $|1\rangle$, $|2\rangle$ and $|3\rangle$, $|4\rangle$ of Figure 6 with HF g-sublevels $F'' = 1$, $F'' = 2$ and e-sublevels $F' = 2$, $F' = 3$, accordingly, in the case of Na atoms (see Figure 1), while, for Cs HF structure, we choose HF g-sublevels $F'' = 3$, $F'' = 4$ and e-sublevels $F' = 4$. $F' = 5$.
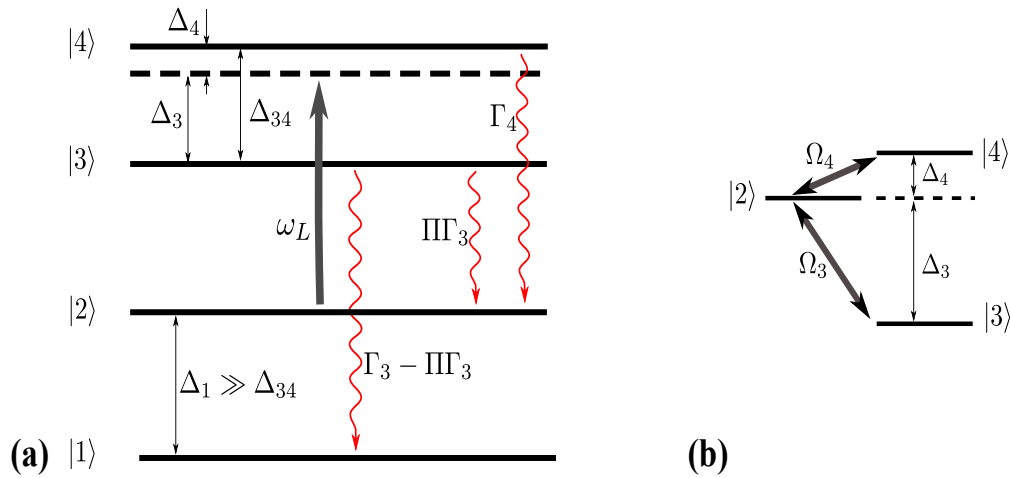


**Figure 6.** (**a**) schematic illustration of a three-level system having a cyclic transition $|4\rangle \rightarrow |2\rangle$ and a partially open transition $|3\rangle \rightarrow |2\rangle$ with the branching factor $\Pi$. The additional passive state $|1\rangle$ accumulates the population due to the spontaneous transition $|3\rangle \rightarrow |1\rangle$; (**b**) the same scheme in the rotating wave approximation. The bare ground state $|2\rangle$ is selected as the position of zero energy (dashed horizontal line).

We are concerned here with the resonant excitation of cyclic HF transitions between HF sublevels. As a consequence, we set the following constrains for laser detuning $\delta = \omega_L - \omega_{42}$, as indicated in Figure 6: $\delta = -\Delta_4 \sim \Gamma << \Delta_3 \approx \Delta_{34}$, where $\Gamma = \Gamma_3 = \Gamma_4$ is the unique natural linewidth of the upper $n^2 p_{3/2}$ levels. The lower levels $|1\rangle, |2\rangle$ correspond to the HF sublevels of the ground state $n^2 s_{3/2}$. Its large HF splitting ($\Delta_1$), compared to the one ($\Delta_{34}$) of resonant states $n^2 p_{3/2}$, transforms the state $|1\rangle$ into a dark state that is not interacting with the pump laser. Figure 6b shows the dressed state configuration obtained using the rotating wave approximation [14]. If the energy $\varepsilon_2$ of the state 2 is chosen as zero, then the energies $\varepsilon_{3,4}$ of the dressed states $|3\rangle, |4\rangle$ turn out to be determined by the laser detuning $\delta$: $\varepsilon_4 = \Delta_4 = -\delta$, $\varepsilon_3 = -\Delta_3$.

It is convenient to represent the Rabi frequencies $\Omega_{F''F'}$ of the pump laser in terms of a single reduced frequency $\Omega_{red}$ [15], which is the product of the amplitude $A_0$ of the laser field and the reduced dipole matrix element $D_{S,P} = (n^2 S_{1/2} ||D|| n^2 P_{3/2})$ [24] for the respective non HF resolved fine transition: $\Omega_{red} = A_0 D_{S,P}$. The partial Rabi frequency values $\Omega_{F''F'}$ for HF transitions $S_{1/2}, F'' \rightarrow P_{3/2}, F'$ are determined by the corresponding, so-called, line strengths $S_{F''F'}$ [24]:

$$\Omega_{F''F'} = \Omega_{red} \sqrt{\tilde{S}_{F''F'}}; \quad \tilde{S}_{F''F'} = S_{F''F'}/D_{S,P}^2. \tag{8}$$

The values of non-dimensional parameters $\tilde{S}_{F''F'}$ are reported within rectangular frames in Figure 1. In Figure 6b, and subsequent discussions, we are using the abbreviations $\Omega_i = \Omega_{2''i'}$ ($i = 3, 4$).

A fundamentally new aspect for the three-level system is the appearance of the dynamic (AC) Stark shifts [13,14] of the state 2, due to its laser induced mixing with the state 3. As a result, the energy defect (detuning) between states 4 and 2 is also undergoing a shift (see also below, Equation (16))

$$\Delta_4 \rightarrow \delta_4 = \Delta_4 - \Omega_3^2/(4\Delta_{34}). \tag{9}$$

In the case of a resonance ($\Delta_4 = 0$), the increase of the pump laser intensity leads to an increasing shift of the actual detuning $\delta_4$. It is worth noting that, in order to significantly affect the light-induced

asymmetry in the line profile, the absolute value $|\delta_4|$ of detuning must be larger than the natural linewidth $\Gamma$, i.e., according to Equation (9), it is necessary that $\Omega_3$ exceeds the saturation threshold: $\Omega_3^2 > 2\Gamma\Delta_3 > \Gamma^2$.

In the weak excitation limit ($\Omega_4 < \Gamma$), the induced transitions $|2\rangle \rightarrow |4\rangle$ and $|2\rangle \rightarrow |3\rangle$ are independent from each other, as they are relatively weak compared to spontaneous transitions. This means that, due to the partially open $|2\rangle \rightarrow |3\rangle$ transition, the ground state depletion should take place and, consequently, the cyclic transition $|2\rangle \rightarrow |4\rangle$ should be affected by the depletion broadening. The results of Section 2 are applicable for the partially open transition $|2\rangle \rightarrow |3\rangle$. In particular, using the notation of Figures 1 and 3, the relation (2) can be rewritten as

$$\frac{\tau_{pum}}{\tau_{tr}} \approx \frac{1}{\tau_{tr}\Gamma_{pum}} = \frac{\tau/\tau_{tr}}{1-\Pi}\frac{4\Delta_3^2}{\Omega_3^2}. \tag{10}$$

The inequality $\tau_{tr}/\tau_{pum} > 1$ characterizing the onset of optical pumping is fulfilled at $\Omega_3 > \Omega_{cr}$ = 1.50 MHz and $\Omega_3 > \Omega_{cr}$ = 9.6 MHz for Na and Cs, respectively, for the experimental ratio $\tau_{tr}/\tau \sim 10^4$. It is well seen that, in the case of Cs, its critical value $\Omega_{cr}$ lies beyond the saturation threshold. At such Rabi frequencies, the linear approximation is no longer applicable and a more accurate approach is required to describe the light–matter interaction.

### 4.1. Adiabatic Approach

The large value of the ratio $\tau_{tr}/\tau \sim 10^4$ allows one to use the method of adiabatic elimination [14,25] to obtain explicit qualitative description of the above effects for cyclic transitions. The exact analysis of the dynamics of optical pumping should be carried out within the framework of the density matrix [14] for the three-level system model shown in Figure 6b. Equations describing the interaction of a single atom (from the atomic beam) with a classical exciting radiation are the optical Bloch Equations [14]:

$$i\dot{\rho}_{ij} = \omega_{ij}\rho_{ij} + \sum_k \left( H_{ik}\,\rho_{kj} - \rho_{ik}\,H_{kj} \right) + il_{ij}, \tag{11}$$

where non-diagonal elements $\rho_{ij}$ ($i \neq j$) are associated with the so-called coherence while diagonal elements give the level population $n_i : n_i = \rho_{ii}$. The matrix $l_{ij}$ describes relaxation processes due to spontaneous radiative transitions. The matrix $H_{ik}$ determines the interaction of atoms with the laser light. If the electric field of the excitation laser in Figure 3 has a Gaussian distribution, $E(z) = A_0 \exp(-z^2/(2d^2))$, with width $d$ along the atomic beam axis (coordinate $z$), then in the rotating wave approximation (RWA) [14] $H_{ik}$ has the following representation (see also Equation (8)):

$$\Omega_{F''F'}(t) = 0.5 \cdot \Omega_{red}\sqrt{\tilde{S}_{F''F'}}\exp(-2t^2/\tau_{tr}^2). \tag{12}$$

The time of flight of an atom through the excitation zone is determined by the laser beam waist size $d$: $\tau_{tr} = 2\,d/v$. Under the experimental conditions of [12], the respective values are $\tau_{tr} \approx 1.1$ mm and $\tau_{tr} \approx 200$ μs.

It is worth noting that all individual members of Equation (12) may be rewritten in the universal form:

$$\dot{X}_k = -\left(\Gamma_k + i\omega_k\right)X_k + F_k(t). \tag{13}$$

Equation (13) can be interpreted as the equation of a linear oscillator with complex coordinates $X_k$, which are subject to a slowly varying external force $F_k(t)$. One can see that the frequency detuning $\omega_k$ plays the role of rigidity, while the width $\Gamma_k$ is associated with the dissipation constant. From classical mechanics, it is well known that characteristic time $\tau_{rel}$ of the evolution of a forced oscillator

to a steady-state condition is determined as $\tau_{rel} = 1/\sqrt{\Gamma_k^2 + \omega_k^2}$ [26]. If $\tau_{tr} >> \tau_{rel}$, the left-hand side of Equation (13) becomes negligible, so that Equation (13) has the following solutions:

$$X_k = F_k(t) / (\Gamma_k + i\omega_k) \, ; \tau_{tr} >> 1/\sqrt{\Gamma_k^2 + \omega_k^2}. \tag{14}$$

*4.2. Strict Results*

Adiabatic elimination for Bloch equations (11) was implemented in [27]. At the first stage, using Equation (14), we express non-diagonal elements $\rho_{ij}$ $(i \neq j)$ via diagonal ones, i.e., via populations $n_i$. As a result, the following closed equation systems describe the population dynamics:

$$\dot{n}_2 = \Gamma n_4 + \Gamma \Pi n_3 + r_4(n_4 - n_2) + r_3(n_3 - n_2), \tag{15a}$$

$$\dot{n}_i = -\Gamma n_i - r_i(n_i - n_2); \quad i = 3, \, 4, \tag{15b}$$

$$r_i = \Omega_{i2}^2 \frac{\Gamma_i}{4\delta_i^2 + \Gamma_i^2}, \quad \delta_i = \omega_{i2} - \frac{\Omega_{j2}^2}{4\omega_{43}}, \quad \Gamma_i = \Gamma\left(1 + \frac{\Omega_{j2}^2}{2\omega_{43}^2}\right), \quad j \neq i, 2, \tag{16}$$

where $\omega_{43}$ is the difference between energies $\varepsilon_4$ and $\varepsilon_3$. These relations have the structure of balance equations for population transfer between the levels due to the spontaneous, with rate $\Gamma$, and laser stimulated, with rate $r_i$, transitions. An important result is the appearance of the AC Stark shifts $\Omega_{j2}^2/(4\omega_{34})$ (see also Equation (9)) in the pumping rate constant $r_i$.

Owing to the adiabatic elimination, system (15) can be further reduced to a single equation for the total population $N(t)$ $(N = n_2 + n_4 + n_3)$ [25] of a single atom:

$$\dot{N} = -\frac{\Gamma \cdot (1 - \Pi) \cdot r_3}{\Gamma + 2r_3 + r_4 \left(\Gamma + r_3\right) / \left(\Gamma + r_4\right)} N, \tag{17}$$

$$n_2 = \frac{N}{1 + r_4/\left(\Gamma + r_4\right) + r_3/\left(\Gamma + r_3\right)}; \quad n_i = \frac{r_i}{\Gamma + r_i} n_2 \quad i = 3, 4. \tag{18}$$

This reduction allows us to obtain an explicit representation for the fluorescence signal $J$, which is proportional to the total number $\Gamma(\bar{n}_4 + \bar{n}_3)$ of photons emitted by a single atom from the excitation volume

$$J = J(t)\,|_{t=\infty} \equiv \Gamma \int_{-\infty}^{t} d\tau \cdot (n_4(\tau) + n_3(\tau))\,|_{t=\infty}. \tag{19}$$

*4.3. Discussion of the Line–Shape Structure*

Solid lines in Figures 4 and 5 are plotted using Formula (19). Note that the theoretical results well describe the experimental data. Both profiles for Na and Cs atoms have an asymmetry, manifested in a rapid drop of the right wings. This asymmetry is due to the upwards AC Stark energy shift (see Equations (9) and (16)) of level $| \, 2 \rangle$ in Figure 6, which corresponds to the HF sublevel $F'' = 2$ for Na and $F'' = 4$ for Cs. As a result, the value of actual detuning $\delta_4 = \Delta_4 - \Omega_3^2/\Delta_{43}$ depends on the sign of $\Delta_4 = -\delta$, i.e., the actual detuning $\delta_4$ for the same absolute value of laser detuning $\delta$ is larger for the right wing side compared to the left wing side.

There is another point that complicates the situation. The structure of Equation (17) implies a slow decay of the population resulting from a weak laser stimulated mixture between states $| \, 2 \rangle$ and $| \, 3 \rangle$. It means the cyclic transition $| \, 2 \rangle \rightarrow | \, 3 \rangle$ ceases to be closed. The decay factor should manifest itself in a depletion broadening. The actual profile, thus, is formed via interplay of space dependent (see Equations (16) and (17)) optical pumping and AC Stark effects.

## 5. Conclusions

One of the characteristic features of a cold medium is the long interaction time $\tau_{tr}$ between light and atoms. As a result, a variety of nonlinear optical effects may take place even for moderate values of light power. We have experimentally observed and theoretically modeled such nonlinear effects by studying HF-selective laser interaction with cold atomic beams consisting of alkali atoms.

Significant modifications of the optical features are found in closed transitions. In particular, we have predicted and experimentally demonstrated the appearance of an asymmetry in the corresponding absorption lines and have explained this occurrence through AC Stark shifts of the involved states. The long transit time ($\sim$0.2 ms) through the excitation zone, combined with a relatively small mixing of HF sublevels of the resonant $n^2p_{3/2}$ state due to the laser coupling results in opening a decay channel for cyclic transitions. The particularities of the line shape formation are a result of the strong interplay between time dependent optical pumping and AC Stark effects.

The results discussed here are of potential interest for interpretation of spectroscopic data obtained from fluorescence spectra of a cold medium of astrophysical relevance such as different modifications of cold white dwarfs or neutral sodium clouds near Jovian moon Io.

**Author Contributions:** F.F. conceived, designed and performed the experiments; A.N.K. contributed analysis tools; V.A.S. analyzed the data, D.K.E. and M.B. performed the calculations; N.N.B., M.S.D., M.B. and Y.N.G. wrote the paper.

**Conflicts of Interest:** The authors declare no conflict of interest.

## References

1. Debes, J.H.; Walsh, K.J.; Stark, C. The link between planetary systems, dusty white dwarfs, and metal-polluted white dwarfs. *Astrophys. J.* **2012**, *747*, 148–156. [CrossRef]
2. Gianninas, A.; Dufour, P.; Kilic, M.; Brown, W.R.; Bergeron, P.; Hermes, J. Precise atmospheric parameters for the shortest-period binary white dwarfs: gravitational waves, metals, and pulsations. *Astrophys. J.* **2014**, *794*, 35–52. [CrossRef]
3. Chary, R.; Zuckerman, B..; Becklin, E.E. *Observational Constraints on the Origin of Metals in Cool DA-Type White Dwarfs*; The Universe as Seen by ISO; Cox, P., Kessler, M., Eds.; ESA Special Publication: Noordwijk, The Netherlands, 1999, Volume 427, pp. 289–291. [astro-ph/9812090].
4. Dupuis, J.; Fontaine, G.; Wesemael, F. A study of metal abundance patterns in cool white dwarfs. III-Comparison of the predictions of the two-phase accretion model with the observations. *Astrophys. J. Suppl. Ser.* **1993**, *87*, 345–365. [CrossRef]
5. Xu, S.; Jura, M. The Drop during Less than 300 Days of a Dusty White Dwarf's Infrared Luminosity. *Astrophys. J. Lett.* **2014**, *792*, L39. [CrossRef]
6. Shvartzvald, Y.; Yee, J.; Novati, S.C.; Gould, A.; Lee, C.U.; Beichman, C.; Bryden, G.; Carey, S.; Gaudi, B.; Henderson, C.; et al. An Earth-mass Planet in a 1 au Orbit around an Ultracool Dwarf. *Astrophys. J. Lett.* **2017**, *840*, L3. [CrossRef]
7. Brown, R.A. Optical Line Emission from Io. In *Exploration of the Planetary System*; Woszczyk, A., Iwaniszewska, C., Eds.; IAU Symposium: Paris, France 1974; Volume 65, pp. 527–531. [CrossRef]
8. Brown, R.A.; Chaffee, F.H., Jr. High-resolution spectra of sodium emission from Io. *Astrophys. J.* **1974**, *187*, L125–L126. [CrossRef]
9. Wilson, J.K.; Mendillo, M.; Baumgardner, J.; Schneider, N.M.; Trauger, J.T.; Flynn, B. The dual sources of Io's sodium clouds. *Icarus* **2002**, *157*, 476–489. [CrossRef]
10. Mendillo, M.; Baumgardner, J.; Flynn, B.; Hughes, W.J. The extended sodium nebula of Jupiter. *Nature* **1990**, *348*, 312–314. [CrossRef]

11. Porfido, N. A Slow and Cold Particle Beam for Nanotechnological Purposes. Ph.D. Thesis, Pisa University, Pisa, Italy, 2012.

12. Porfido, N.; Bezuglov, N.; Bruvelis, M.; Shayeganrad, G.; Birindelli, S.; Tantussi, F.; Guerri, I.; Viteau, M.; Fioretti, A.; Ciampini, D.; et al. Nonlinear effects in optical pumping of a cold and slow atomic beam. *Phys. Rev. A* **2015**, *92*, 043408. [CrossRef]

13. Metcalf, H.J.; Van der Straten, P. *Laser Cooling and Trapping*; Springer: New York, NY, USA, 1999.

14. Shore, B.W. *Manipulating Quantum Structures Using Laser Pulses*; Cambridge University Press: Cambridge, UK, 2011.

15. Sydoryk, I.; Bezuglov, N.; Beterov, I.; Miculis, K.; Saks, E.; Janovs, A.; Spels, P.; Ekers, A. Broadening and intensity redistribution in the Na (3p) hyperfine excitation spectra due to optical pumping in the weak excitation limit. *Phys. Rev. A* **2008**, *77*, 042511. [CrossRef]

16. Bezuglov, N.; Ekers, A.; Kaufmann, O.; Bergmann, K.; Fuso, F.; Allegrini, M. Velocity redistribution of excited atoms by radiative excitation transfer. II. Theory of radiation trapping in collimated beams. *J. Chem. Phys.* **2003**, *119*, 7094–7110. [CrossRef]

17. Beterov, I.; Tretyakov, D.; Ryabtsev, I.; Bezuglov, N.; Miculis, K.; Ekers, A.; Klucharev, A. Collisional and thermal ionization of sodium Rydberg atoms III. Experiment and theory for nS and nD states with $n = 8$–$20$ in crossed atomic beams. *J. Phys. B* **2005**, *38*, 4349–4361. [CrossRef]

18. Miculis, K.; Beterov, I.; Bezuglov, N.; Ryabtsev, I.; Tretyakov, D.; Ekers, A.; Klucharev, A. Collisional and thermal ionization of sodium Rydberg atoms: II. Theory for nS, nP and nD states with $n = 5$–$25$. *J. Phys. B* **2005**, *38*, 1811–1831. [CrossRef]

19. Zakharov, M.Y.; Bezuglov, N.; Lisenkov, N.; Klyucharev, A.; Beterov, I.; Michulis, K.; Ékers, A.; Fuso, F.; Allegrini, M. Optimization of sub-Doppler absorption contour in gas-dynamic beams. *Optic. Spectrosc.* **2010**, *108*, 877–882. [CrossRef]

20. O'Dwyer, C.; Gay, G.; de Lesegno, B.V.; Weiner, J.; Camposeo, A.; Tantussi, F.; Fuso, F.; Allegrini, M.; Arimondo, E. Atomic nanolithography patterning of submicron features: writing an organic self-assembled monolayer with cold, bright Cs atom beams. *Nanotechnology* **2005**, *16*, 1536–1541. [CrossRef]

21. Camposeo, A.; Piombini, A.; Cervelli, F.; Tantussi, F.; Fuso, F.; Arimondo, E. A cold cesium atomic beam produced out of a pyramidal funnel. *Opt. Commun.* **2001**, *200*, 231–239. [CrossRef]

22. Bezuglov, N.; Molisch, A.; Fioretti, A.; Gabbanini, C.; Fuso, F.; Allegrini, M. Time-dependent radiative transfer in magneto-optical traps. *Phys. Rev. A* **2003**, *68*, 063415. [CrossRef]

23. Bezuglov, N.; Molisch, A.; Fuso, F.; Allegrini, M.; Ekers, A. Nonlinear radiation imprisonment in magneto-optical vapor traps. *Phys. Rev. A* **2008**, *77*, 063414. [CrossRef]

24. Sobelman, I.I. Radiative Transitions. In *Atomic Spectra and Radiative Transitions*; Springer: Berlin, German, 1992; pp. 200–302.

25. Stenholm, S. *Foundations of Laser Spectroscopy*; Courier Dover: New York, NY, USA, 2005.

26. Landau, L.; Lifshits, E. *Mechanics*; Pergamon Press: New York, NY, USA, 1969.

27. Bruvelis, M.; Cinins, A.; Leitis, A.; Efimov, D.; Bezuglov, N.; Chirtsov, A.; Fuso, F.; Ekers, A. Particularities of optical pumping effects in cold and ultra-slow beams of Na and Cs in the case of cyclic transitions. *Optic. Spectrosc.* **2015**, *119*, 1038–1048. [CrossRef]